European Polymer Journal 46 (2010) 112–122

Contents lists available at ScienceDirect

European Polymer Journal

journal homepage: www.elsevier.com/locate/europolj

Monte Carlo study of the translocation of a polymer chain through a hole

Waldemar Nowicki [a,*], Grażyna Nowicka [a], Jolanta Narkiewicz-Michałek [b]

[a] Faculty of Chemistry, Adam Mickiewicz University, Grunwaldzka 6, 60-780 Poznań, Poland
[b] Faculty of Chemistry, Maria Curie-Skłodowska University, M. Skłodowska-Curie Pl. 3, 20-031 Lublin, Poland

ARTICLE INFO

Article history:
Received 27 March 2009
Received in revised form 16 September 2009
Accepted 11 October 2009
Available online 10 November 2009

Keywords:
Self-avoiding walk
Excluded volume
Surface curvature
Athermal solution

ABSTRACT

The translocation of a polymer chain through a narrow hole in a rigid obstacle has been studied by the static Monte Carlo simulations. A modified self-avoiding walk on a cubic lattice has been used to model the polymer in an athermal solution. The entropy of the chain before, in the course, and after the translocation process has been estimated by the statistical counting method. The thermodynamic generalized forces governing the translocation have been calculated. The influence of the system geometry on the entropic barrier landscape is discussed.

1. Introduction

The passage of a macromolecule through a nanometer-size pore is a fundamental event in various biological processes including protein translocation across membranes [1,2], gene transduction between bacteria [3] and the introduction of viral DNA to the cytoplasm of bacterial cell [4]. In addition to its biological relevance, this process is of key importance in a growing number of applications, like drug delivery [5], ultrarapid DNA sequencing [6], separation and purification of synthetic and biological polymers [7,8], to name a few.

The polymer chain threading through a nanopore is a complicated phenomenon. It has been extensively studied both by theoretical and simulation methods. The threading of the chain is usually induced by the external force. Several effects have been considered as sources of driving forces of the translocation process: the electrostatic interaction between charged macromolecules and the external electric field [9–11], the gradient of the chemical potential in the direction parallel to the nanopore axis [12,13], the difference in the Flory–Huggins interaction parameters between the solutions on both sides of a nanoporous membrane [14], the entropic force arising from the spatial confinement imposed on the polymer chain [15–17], the selective adsorption of polymer on one side of the membrane [18–21], the curvature-induced difference of lipid fluctuations between the two halves of the bilayer (in the case of the translocation through a curved membrane) [22], the ratchet mechanism [23], et cetera.

Threading a polymer through a narrow nanopore was modelled by various methods. The translocation of the polymer molecule through the nanopore placed in the external field was studied via molecular dynamics method [9,10], Brownian dynamics simulation [12,24], Langevine dynamics simulation [25], dissipative particle dynamics method [26] and others. The translocation problem was also frequently addressed by different modifications of 2D and 3D dynamic Monte Carlo (MC) simulations [18,22,27–34]. Results of different simulations allow formulation of some conclusions concerning dynamic features of translocation, i.e. the macromolecule velocity [35,36], kinetic equations of the translocation process [14], dependence of translocation time on the polymer length [30,32,33], chain diffusion coefficient [22,36]. The simulations indicated the presence of two different regimes of translocation dynamics depending on the ratio of the pore to polymer lengths as well as two different re-

* Corresponding author.
E-mail address: gwnow@amu.edu.pl (W. Nowicki).

0014-3057/$ - see front matter © 2009 Elsevier Ltd. All rights reserved.
doi:10.1016/j.eurpolymj.2009.10.012

gimes for the probability of translocation depending on the voltage applied [9]. Also, the influence of temperature on the translocation time was extensively studied [9,10,32]. The anomalous dynamics of translocation was discussed by Kantor and Kardar [37]. Simulations of the translocation through a nanopore in the absence of an external driving force were performed by the 2D MC method [25,28] for the system containing a chain initially situated in the middle of the pore. The escape time required for the polymer to completely exit the pore was studied. The MC simulations were also used for investigations of distribution of charged and neutral polymers with different flexibilities between two spheres of varying volume, connected by a short and narrow cylinder [27]. Also, the translocation in systems containing many macromolecules was considered [29].

An important quantity describing the chain translocation process is the height of the Helmholtz free energy barrier which has to be overcome in the course of the translocation. However, full understanding of the physical backgrounds of the process needs the information about details of the entire landscape of free energy [38].

The main objective of the paper was to estimate the excess free energy of the chain translocation at all steps of the process and, as a consequence, to calculate the thermodynamic generalized forces produced by the confining environment of the chain in the course of the chain translocation. The information about these forces is of importance because it allows anticipation of the external forces necessary to induce the translocation. Using the static Monte Carlo (MC) method [39] and the statistical counting (SC) method [40] we have studied a system of a single isolated polymer chain restricted into geometrical constrains. The chain was represented by the modified self-avoiding walk ((1 1 2) SAW) [41], thus the model can be related to the properties of a macromolecule in an athermal solution, where the crucial quantity, fully determining the system properties, is the conformational entropy. The method applied does not allow a direct study of the translocation dynamics. Nevertheless, it can be employed for the computation of the conformational entropy at all steps of the translocation and for numerical calculations of partial derivatives of entropy with respect to distance and volume, corresponding to the generalized thermodynamic forces – the mechanical force and pressure.

In this study we calculated exact values of the free energy of the system governed only by excluded volume effects. Nevertheless, these values can be also interpreted as the entopic components of free energy in more complicated systems governed by strong interactions (e.g. electrostatic potentials).

2. Model

2.1. Chain translocating through a hole

In order to calculate the entropy of a linear polymer chain in the course of translocation through a small hole we applied the results of computation of the conformational entropy of the chain terminally attached to the surface, in details described in [41]. Instead of the standard SAW model, in which each segment links two nearest lattice nodes [42], we used the algorithm, in which the segments of the chain were connected by vectors of the type $[\pm a, \pm a, \pm 2a]$, $[\pm a, \pm 2a, \pm a]$ and $[\pm 2a, \pm a, \pm a]$ and the length equal to $\sqrt{6}a$. Further in the text, this algorithm is referred to as the (1 1 2) motion. A fragment of the chain generated by this algorithm is shown in Fig. 1. This generation method is similar to those applied for simulations of polypeptides, where (1 2 3) and (0 2 3) algorithms were used [34,43], and gives the coordination number ω equal to 24. Such a high value of ω results in a very large flexibility of the chains generated. Below, we present brief information on the calculation method.

The entropies of attached chains were obtained by means of the static Rosenbluth–Rosenbluth MC method [39,42] on a 3D cubic lattice of a lattice constant a. The simulations were performed in a box containing one linear chain and obstacles of flat or curved surfaces. In most simulations, chains of 1000 segments were considered. Each polymer segment occupied one lattice site. No interactions were considered in the model except the excluded volume of the polymer chains and the obstacles. In consequence, the system modelled the athermal solution [44]. The conformational entropy of the SAW chain was calculated by means of the SC method [40].

In the present paper, we assumed that the system consisted of two parts represented by half-spaces or by spherical donor of the radius R and recipients of different geometries, as shown in Fig. 2. The donor and recipient spaces were joined by a narrow hole in the separating wall. The polymer thread was assumed to be in the course of the translocation process through the hole. The hole size was of one lattice site and the wall thickness around the hole was of that of a layer of the lattice. Hence, the segment just passing through the hole could not change its position in the direction parallel to the wall and at any moment of the translocation process the polymer chain could be considered as a system of two independent chains end-tethered to opposite sides of the wall. Consequently, at a certain moment of the process the conformational entropy S of the whole translocating chain composed of N segments

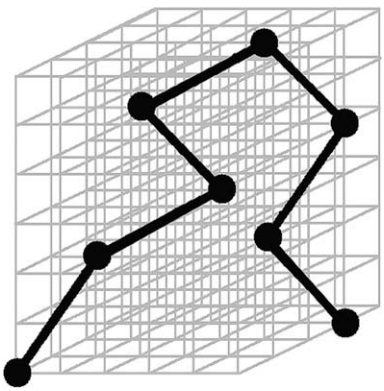

Fig. 1. Visualization of the (1 1 2) SAW on a 3D cubic lattice. Circles denote lattice sites blocked by segments connected by bonds generated by means of (1 1 2) algorithm.

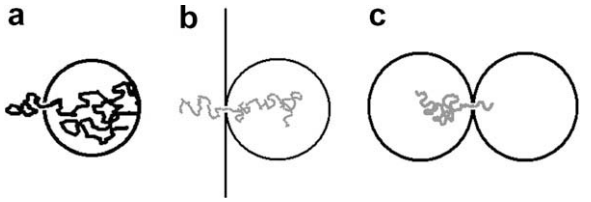

Fig. 2. Schemes of three different geometries of systems for the study of chain translocation: (a) a hollow sphere, (b) a spherical cavity cored in a flat wall, (c) interconnected twin cavities.

can be obtained by the summation of the corresponding entropies of its two sections:

$$S = S(N_1) + S(N_2) = S((1-\zeta)N) + S(\zeta N) \quad (1)$$

where N_1 and N_2 denote the numbers of segments in the chain sections being in the opposite sides of the hole and ζ is the chain partition ratio used as the translocation coordinate and defined as:

$$\zeta = \frac{N_2}{N_1 + N_2} \quad (2)$$

The entropy change accompanying the chain translocation can be expressed as:

$$\Delta S = S(N_1) + S(N_2) - S(N) \quad (3)$$

where $S(N)$ corresponds to the entropy of the end-tethered chain.

2.2. Chain located near the interface

The chain behaviour just before and soon after the translocation through the hole was investigated in the way similar to that described in Section 2.1 with the difference that instead of the chain attachment to the surface, two other types of space constraints were applied. The first constraint applied corresponded to the deformation of the coil forced by the vicinity of the surface. In these independent simulations, the walk started at a lattice site located at a distance d from the surface. Another constraint modelled the capturing of the whole chain into the spherical cavity of a radius R. In this case the generation of each chain started at a lattice site randomly chosen from all sites located inside the cavity. The chain propagation came under the same (1 1 2) SAW rules as described in Section 2.1.

Each data set presented in the paper was calculated as an average of results obtained from 10^5 chain conformations.

3. Results

3.1. Translocation through a hole in flat wall

The translocation of a polymer chain through a nanopore faces a large entropic barrier due to the loss of a great number of available configurations. As mentioned above, the conformational entropy of the chain can be calculated as the sum of entropies of two independent chains end-tethered to the opposite sides of the wall (Eq. (3)). Since the difference between the conformational entropy of the chain attached through its terminal segment to the flat surface and that of a free chain can be expressed for relatively short chains by the simple power law [41]:

$$\frac{\Delta S}{k_B} = -H_1\sqrt{N} \quad (4)$$

with H_1 equal to 0.650 ± 0.002, one can suppose that ΔS of the chain passing through a hole in the flat wall can be expressed by the equation following from the power law (Eq. (4)):

$$\frac{\Delta S}{k_B} = -H_2\sqrt{N}(\sqrt{1-\zeta} + \sqrt{\zeta} - 1) \quad (5)$$

where the prefactor H_2 obtained by the fitting procedure is equal to 0.44 ± 0.01.

Eq. (5) gives the minimum value of the translocation entropy at the translocation coordinate ζ equal to 1/2, e.g. when $N_1 = N_2$. For $\zeta \to 0$ or $\zeta \to 1$, the chain tends to the conformation perturbed only by the attachment of the terminal segment to the interface and the entropy of translocation reaches zero.

The results of simulations obtained for a chain of $N = 1000$ together with the results of Eq. (5) are shown in Fig. 3. As seen, there is a satisfactory agreement between the simulation and the theoretical curves.

It is noteworthy that the prefactor in Eq. (5) is significantly lower than that in Eq. (4), which is due to the screening of the excluded volume effect of both parts of the translocating chain by the wall.

Eq. (5) allows the calculation of the net force F acting along the translocating chain. At a constant temperature

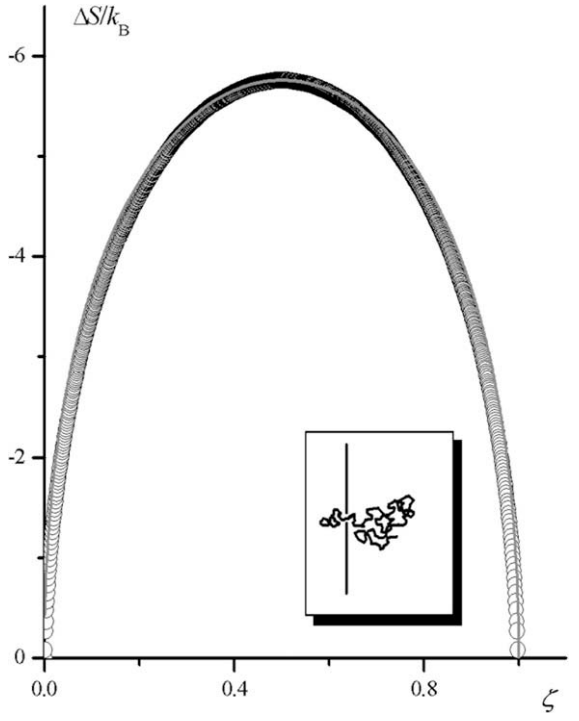

Fig. 3. The dependence of ΔS on ζ for a chain of $N = 1000$ translocating through a hole in a flat wall (simulation results – circles, results of Eq. (5) – a grey line).

T this force is equal to the derivative of the change in free energy upon the translocation, ΔA, with respect to the length x of the chain section which crossed the wall:

$$F = \left(\frac{\partial \Delta A}{\partial x}\right)_T = \left(\frac{\partial const}{\partial x}\right)_T - T\left(\frac{\partial \Delta S}{\partial x}\right)_T = -T\left(\frac{\partial \Delta S}{\partial x}\right)_T = -\frac{T}{Nl}\left(\frac{\partial \Delta S}{\partial \zeta}\right)_T \quad (6)$$

Finally, the following relation between the force F, the translocation coordinate ζ, and the number of segments in the whole chain, N, can be obtained:

$$\frac{Fl}{T} = -\frac{1}{N}\left(\frac{\partial \Delta S}{\partial \zeta}\right)_T = \frac{H_2 k_B}{2\sqrt{N}}\left(\frac{1}{\sqrt{1-\zeta}} - \frac{1}{\sqrt{\zeta}}\right) \quad (7)$$

The dependence between F and ζ, determined on the basis of the simulation results, is presented in Fig. 4. As seen, the dependence crosses zero at $\zeta = 1/2$. At this point the segment currently filling the hole is pulled by two chain sections of the same length, so the net force is equal to zero.

Eq. (7) permits calculation of another interesting quantity – the pulling force exerted by the terminal segment attached to the surface. In order to calculate the force, let's consider the translocating chain at the end of the process, that is a situation where all segments gather at one side of the wall, except the end segment which fills-out the hole and is assumed to represent the grafted segment. At the junction point the chain pulls on the wall by the force which can be found from Eq. (7) when $\zeta \to 0$ or $\zeta \to 1$. As the translocation of polymer chain is a discrete process let's change the argument of the function from the partition ratio ζ to the index i of the segment currently being in the hole. Then, the pulling force reads:

$$F_{att} = \lim_{i\to 1} F = \lim_{i\to 1}\left(\frac{H_1 k_B T}{2l\sqrt{N}}\left(\frac{1}{\sqrt{1-\frac{i}{N}}} - \frac{1}{\sqrt{\frac{i}{N}}}\right)\right) = -\frac{H_1 k_B T}{2l}\left(\frac{\sqrt{N-1}-1}{\sqrt{N-1}}\right) \approx -\frac{H_1 k_B T}{2l} \quad (8)$$

Considering that all segments of the chain are gathered at one side of the wall, the prefactor in Eq. (8) takes the same value as in Eq. (4).

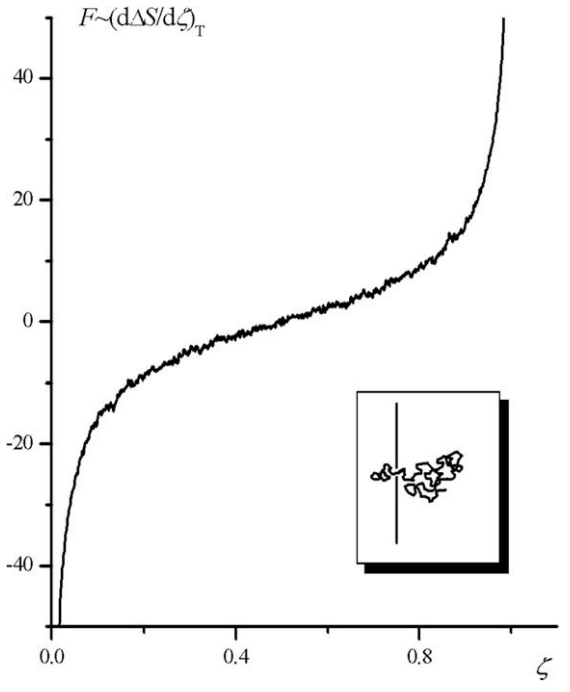

Fig. 4. The dependence of F on ζ for $N = 1000$.

3.2. Escape from a spherical confinement

As mentioned in Section 1, the driving force for the polymer translocation can be generated by various means. It can be also produced, at least in part, by a spatial confinement of the polymer [16,19–21]. The confinement induced reduction of the conformational entropy of the polymer chain results in an excess free energy which drives the escape of the polymer out of the confining space.

The excess free energy depends on the confinement degree of polymer in both donor and recipient spaces. We have calculated changes in the conformational entropy during the chain escape and net forces acting along the escaping chain for three different types of geometry of the donor/recipient system presented in Fig. 2. Formally, the conformational entropies of the whole translocating chains were estimated by the summation of the entropies of its two sections placed in donor and recipient spaces and attached to the wall at the point corresponding to the hole. The results of the calculations are presented in Figs. 5–8.

The influence of the system geometry on the conformational entropy of escaping chain is shown in Fig. 5 in the form of $S/S_{free} = f(\zeta)$ plots (S_{free} stands for the entropy of the free unperturbed chain). As expected, in every case a somewhat different behaviour of the dependencies is observed. The smaller the radius of donor space, the more pronounced the differences. The common feature of the dependencies is the appearance of a minimum (except for very small sphere radii in the case of twin cavities, where the courses of the plots are more complicated), which indicates that the chain escape requires the overcoming of an entropy barrier.

Let us introduce an additional quantity – the relative height of the entropy barrier, defined as: $\Delta S_R = S_{min} - S_{att}$ (where S_{min} denotes the entropy minimum of a chain, achieved in the course of the translocation through the hole, whereas S_{att} is the entropy of the chain terminally attached to the inner surface of the donor sphere). As seen in Fig. 6, the height of the barrier initially increases with the increase in the donor sphere radius; then it tends to the value characteristic of the translocation through the flat wall. The height of the barrier at small R values is governed by the compression of the chain in the cavity and depends only slightly on the system geometry. This indicates that the low entropy of the macromolecule confined in the donor cavity is the main factor promoting the translocation. Moreover, the results presented in Fig. 6 allow formulation

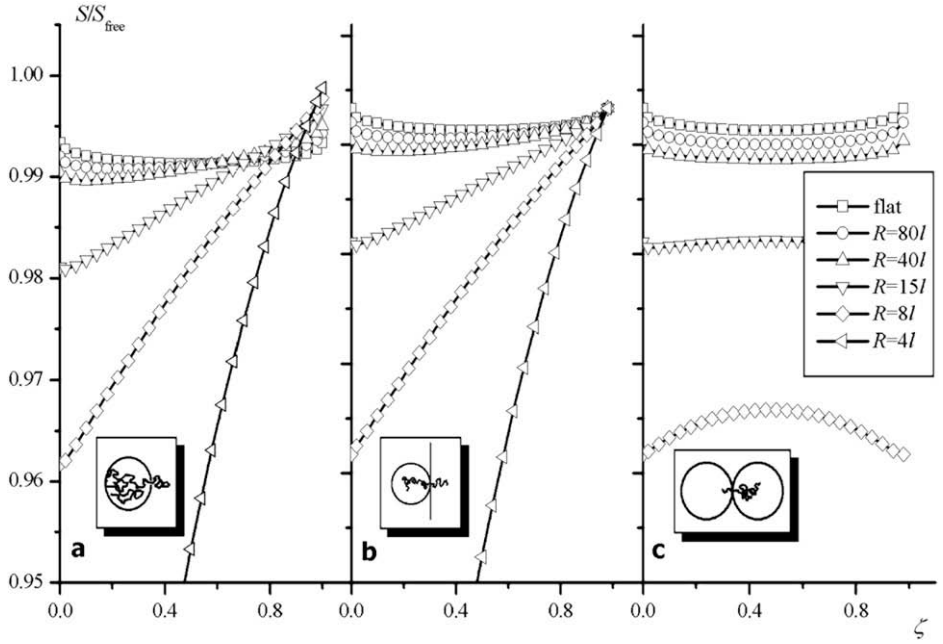

Fig. 5. The influence of the system geometry on the conformational entropy of translocating chain ($N = 1000$) shown in the form of dependencies between S/S_{free} and ζ for different curvature radii of donor cavity (as indicated in figure): (a) the escape outside a hollow sphere, (b) the escape outside a spherical cavity cored in a flat wall, (c) the escape into another spherical cavity of the same size.

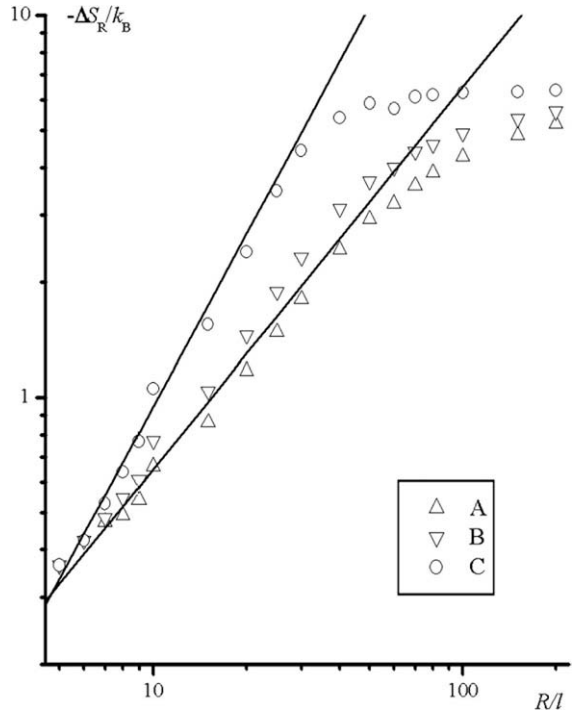

Fig. 6. The effect of the size of the hollow sphere (R) on the relative height of the entropic barrier ($N = 1000$, letters A, B and C indicate the corresponding system geometries, presented in Fig. 2).

of the following power correlation between ΔS_R and R, valid for small R:

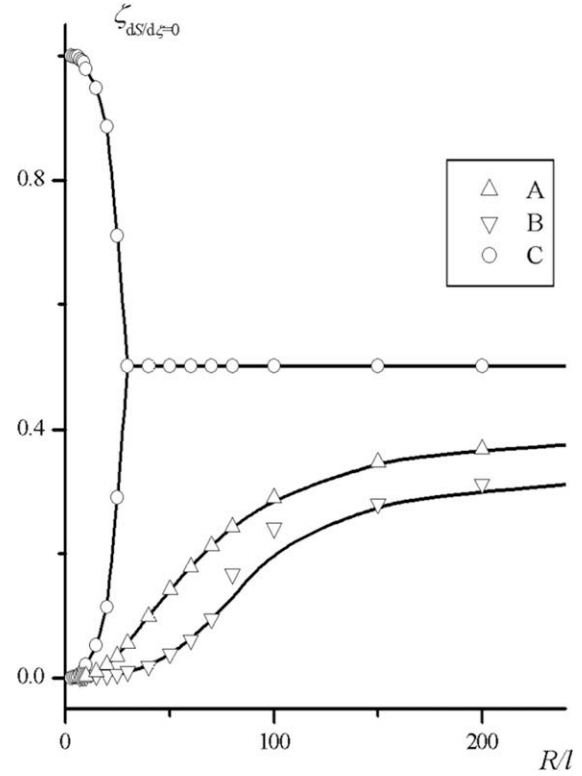

Fig. 7. The effect of the size of the donor sphere on the chain partition ratio at which the net force acting on the chain reaches zero ($N = 1000$, letters A, B and C indicate the corresponding system geometries, presented in Fig. 2).

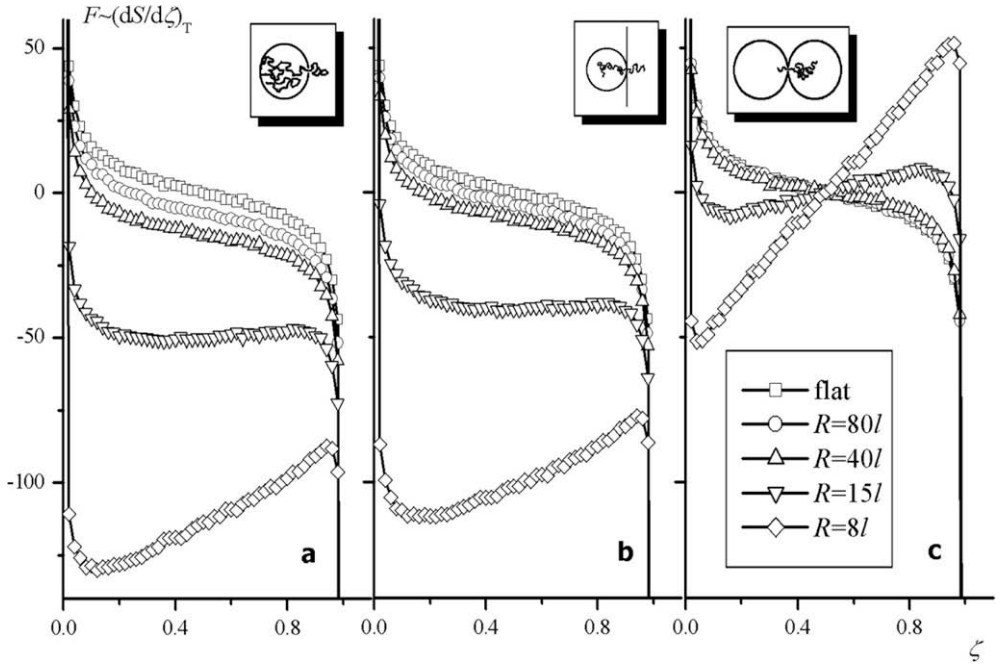

Fig. 8. The influence of the system geometry on the net force acting along the escaping chain ($N = 1000$) shown in the form of dependencies between F and ζ for different curvature radii of donor cavity (all the rest is the same as in Fig. 5).

$$\Delta S_R \sim \left(\frac{R}{l}\right)^b \tag{9}$$

where b is equal to 1.00 ± 0.04 for geometries A and B and to 1.50 ± 0.03 for geometry C. The higher initial slope of the curve obtained for geometry C is a consequence of a fact that the chain translocation from the donor to the recipient sphere causes a decrease in the entropy not only as a result of the imprisonment of the chain in the hole but also as a consequence of the compression of the part of the chain in the recipient sphere.

Fig. 7 shows the relations between the ζ values corresponding to the minima on the S–ζ curves given in Fig. 5 and the donor cavity radii. As seen, for geometries denoted as A and B the character of the dependencies is similar; with increasing R, the position of the minimum increases gradually to $\zeta = 1/2$, which is the value corresponding to a situation where the donor space is the half-space. However, for geometry A (a hollow sphere) the increase is faster.

The S–ζ curves for twin spheres (geometry C, Fig. 5c) are symmetrical with respect to $\xi = 1/2$. For relatively large spheres, where location of the whole chain in the cavity causes negligible small compression, the value of $\zeta = 1/2$ corresponds to the entropy minimum as in the case of the flat wall (compare Fig. 3). However, below a certain critical value of R two symmetrical minima appear (see Fig. 7) as a consequence of the fact that the ΔS of the compression of the chain in the single cavity is comparable with the entropy loss caused by the location of the central segment of the chain in the hole ($\zeta = 1/2$). This implies that the escape of the chain from one sphere into another requires the overcoming of two entropy barriers (two entropy minima), at which the system reaches the metastable state. The minima positions tend to $\zeta = 0$ and $\zeta = 1$ with the decreasing R. The barrier initially present at $\zeta = 1/2$ vanishes since the entropy minimum converts into maximum (see Fig. 5c).

Curves in Fig. 8 illustrate the changes in net force F acting along the chain during the process of the chain escaping. Analysis of these curves indicates that the initiation of the process requires the occurrence of a fluctuation (or an additional force) large enough to shift the chain into a position (described by the separation ratio) where $F \leqslant 0$, then the rest of the process will proceed spontaneously. For geometries A and B, the ζ value for which F reaches zero increases with decreasing R. It means that the smaller the donor radius, the shorter the chain section which has to pass through the hole for the spontaneous escape to be initiated and the more likely that a fluctuation sufficient for the process initiation may happen.

In the case of chain transfer between twin spheres, the force reaches zero at $\zeta = 1/2$ for all R values (curves in Fig. 8c have an anti-symmetrical character). For relatively large spheres, an abscissa of anti-symmetrical centre ($\zeta = 1/2$) indicates the partition ratio of metastable configuration of the chain, whereas for small spheres it points to a stable situation (as there is the symmetrical entropy maximum in Fig. 5c). In the latter case two metastable configurations are also possible, determined by the ζ values corresponding to the entropy minima in Fig. 5c.

3.3. Deformation due to approach to a surface

The results presented in Sections 3.1 and 3.2 concern only a certain stage of the chain translocation process, that is the transition from the situation in which the first seg-

ment is in a hole to the situation in which the last segment is there. However, the approaching of the terminal segment to the hole, as well as the reverse process, that is the withdrawing of the last segment from the hole and moving away of the whole macromolecule far from the wall, also involve a change in the conformational entropy of the polymer.

Upon approaching the wall, the polymer coil undergoes a gradual deformation as compared with its conformation in the absence of the wall. The free polymer coil can be characterized by its linear dimensions: the average radius of gyration, R_G, the end-to-end distance, R_H, the average separation of two the most distant segments ($2R_E$) and the average distance between the coil mass centre and the chain end, Z. The relation between Z and the chain length can be expressed as follows [45]:

$$Z = 6^{-1/4} l N^{\nu} \tag{10}$$

In Fig. 9 the coil is schematically represented as an ellipsoid whose dimensions correspond to $2R_E$. The mean radius of the dark part of the ellipsoid is equal to R_G, whereas the dashed line marks the most probable value of Z. The elimination of a number of possible coil conformations in the vicinity of wall can be considered as a cutting-off of a part of coil peripheries. Thus, the attachment of the terminal segment to the wall can be considered as the approach of wall to the average position of this segment in the coil, as it is schematically presented in Fig. 9. The same figure also illustrates the influence of the surface curvature on the extent of the chain entropy loss induced by the approach of the wall. Moreover, the effect of a temporary anisotropy of the coil, associated with the change in the direction of the end-to-end vector, on this entropy loss can be also seen from Fig. 9.

The entropy penalty accompanying the approach of the end segment to the flat wall was calculated in independent simulations, in which the walk started at a lattice site located at a distance d from the surface of the wall. The simulation results obtained for $N = 1000$ are shown in Fig. 10a, in which the relative conformational entropy of polymer coil versus d is plotted. As seen, with the reduction of the distance d, the gradual decrease in the chain conformational entropy, from the value corresponding to unperturbed coil (S_{free}) to that of terminally attached chain (S_{att}), occurs. The influence of the chain length on the entropy reduction is presented in Fig. 10b, where the ratio $(S–S_{att})/(S_{free}–S_{att})$ is plotted versus d for three different N values. The smaller N, the steeper the curve. This means that when the chain length increases the distance at which the coil perturbation starts to occur also increases or – in other words – at the same value of d the longer the chain, the larger the entropy reduction.

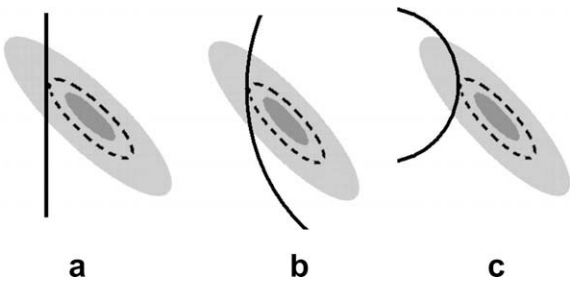

Fig. 9. Ellipsoids representing a polymer coil (see the text for details) and surfaces of different curvatures approaching the average position of end segment in the coil ($R = \infty$ (a); $R < 0$ (b); $R > 0$ (c)).

On the basis of the $S = f(d)$ relationship the entropic force F, which arises upon the coil deformation and counteracts its approach to the wall, was calculated from Eq. (6) for $x = d$. The resulting dependencies $F = f(d)$ obtained for chains of different N differ from each other. However, the shape of the dependencies of F on the relative distance d/R_g (or on $d/N^{3/5}$ as in the case of the athermal solution $R_g \sim N^{3/5}$) is independent of the chain length, as seen in Fig. 11. In the range of small d values ($d < R_G$) the relationship is almost linear and thus it can be expressed by a linear equation:

$$F = F_{att} + \frac{Bd}{N^{3/5}} \tag{11}$$

where B is a constant and F_{att} is the force exerted by the chain terminally attached to the surface equivalent to that expressed by Eq. (8).

The force F_{att} pulls the surface because the escape of the chain from the vicinity of the surface enhances its conformational entropy. Since the surface area on which the pulling force acts is a^2, the pressure exerted by the chain on the wall can be found from the equation:

$$p = \frac{F_{att}}{a^2} \tag{12}$$

As follows from Fig. 11 as well as from Eqs. 8 and 12, both the force F_{att} and the pressure p exerted by the chain in the athermal solution are independent of the segment number in the chain, similarly as in the case of the Gaussian chain [5].

As illustrated in Fig. 12a, due to force balance, the negative pressure p exerted by the terminal segment is accompanied by another positive pressure exerted by the rest of the polymer chain on the wall. In the case of elastic surface (like a biological membrane) the pressure exerted by the macromolecule deforms the surface [46–49]. Bickel et al. [46] calculated the deformation profile for a fluid surface and found that close to the attachment point this profile assumes a cone-like shape, as illustrated in Fig. 12b.

3.4. Deformation due to insertion into spherical cavity

In small cavities the inserted coil can be compressed as compared with its size in the unperturbed state. This compression involves the entropy reduction which produces the entropic pressure exerted by the coil onto the inner surface of the cavity.

In order to consider the effect of coil compression separately, we have generated chains of different N captured inside a sphere of radius R. Each generation started at a point chosen at random inside the sphere. One can expect that the decrease in the cavity radius below the value corresponding to the average radius R_E of the unperturbed coil will cause a gradual decrease in the chain conformational

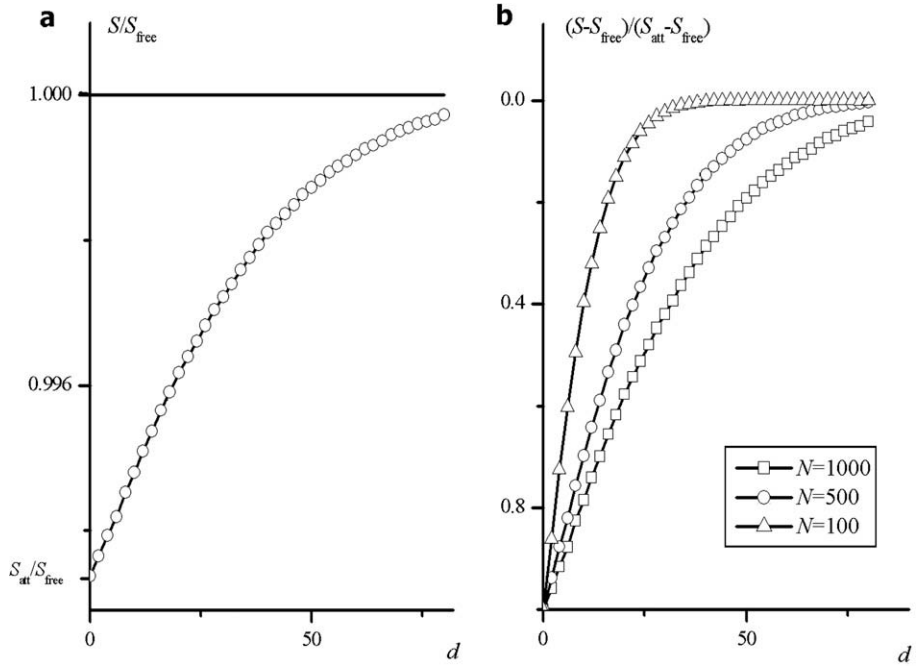

Fig. 10. The influence of d on the relative entropy S/S_{free} of a chain of $N = 1000$ (a), and on the $(S–S_{att})/(S_{free}–S_{att})$ ratio for different N values (as indicated in figure) (b). The horizontal line corresponds to the entropy of unperturbed coil; d is the distance of the terminal segment from the flat wall.

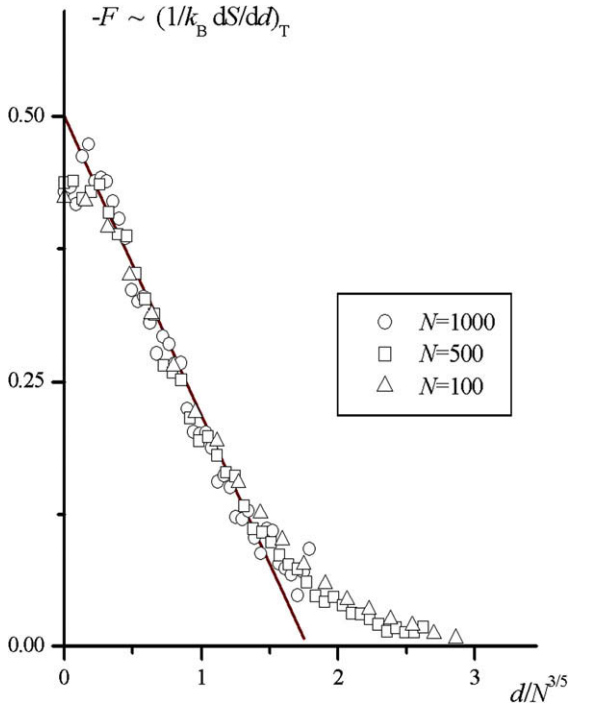

Fig. 11. The dependence of the entropic force opposing the approach of a polymer coil to the flat wall on the relative distance $d/N^{3/5}$ for different chains lengths.

entropy. As expected, the S–R curves obtained for different N and presented in Fig. 13 show that the longer the chain, the greater the entropy loss. The dependence of the entropic pressure on the cavity volume for three different chain lengths is depicted in Fig. 14. The isotherms obtained resemble those of gases and can be expressed by the equation similar to the state equation of the gas of hard spheres:

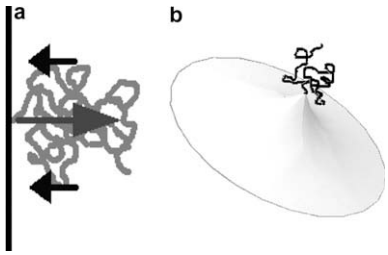

Fig. 12. Entropic forces exerted by an end-grafted chain on a rigid planar wall (a) and the deformation of an elastic surface induced by an end-attached chain (b).

$$p(V - Na^3)^{4/3} \sim N \tag{13}$$

Eq. (13) predicts that for cavity volumes large relative to the excluded volume of the chain, the pressure exerted by the coil scales with the gyration radius of the unperturbed coil and the cavity radius as:

$$p \sim \frac{R_G^{1/\nu}}{R^4} \tag{14}$$

where ν is the Flory's exponent.

3.5. Entire entropy profile

As discussed above, the threading of the polymer chain through a hole in a wall is preceded by the chain approach to and followed by the chain departure from the wall. For the case of a flat wall, the entropy profile of the entire process is presented in Fig. 15, where the values of S/S_{free} are plotted against the chain position relative to the wall. For illustrative purposes, a new parameter $z = \zeta - 1$ is introduced. Let us notice that $z = 0$ corresponds to the situation when the chain is half way through the hole, $|z| = 1/2$ determines the chain with its end segment in the hole and thus $|z| > 1/2$ means that there are no segments being in direct contact with the wall, however only for $|z| > 3/2$ the confining effect of the wall vanishes. As results from Fig. 15, the entropy loss accompanying the approach of the end segment to the wall exceeds by about four times the entropy loss due to the threading of the chain through the hole.

Fig. 16 gives the entire entropy profiles for the chain transfer from spherical cavities of different volumes into the half-space ($R \to \infty$). The profile shapes are not symmetrical with respect to the position of the maximum, which is a consequence of two effects: the curvature dependent entropy reduction caused by the approach of the terminal segment to the hole and the entropy loss due to the chain compression in the cavity. The smaller the cavity volume, the lower the entropy barrier needed to be overcome during the chain translocation and the larger the entropy gain associated with the entire process of the chain transfer from one space to another.

In the case of other geometries represented in Fig. 2 the entire profile of the chain entropy can be easily obtained by combining suitable fragments of $S = f(z)$ dependencies in a way similar to that applied in the construction of Figs. 15 and 16.

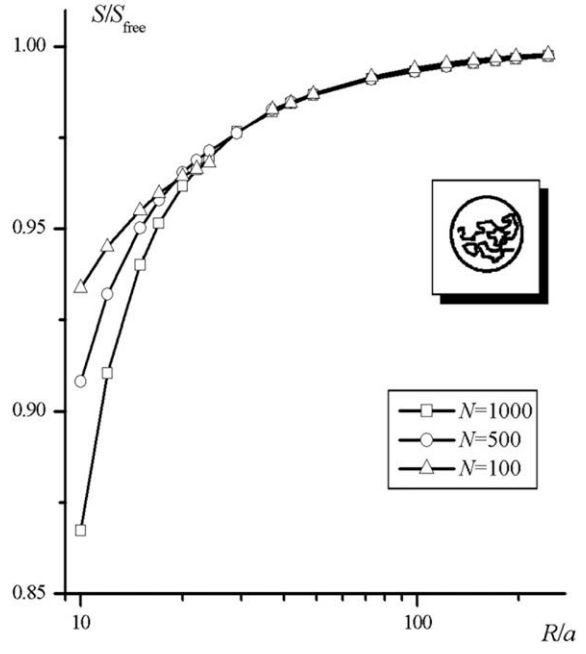

Fig. 13. The influence of sphere radius on the relative entropy of compressed chain, S/S_{free}, for different N values (as indicated in figure).

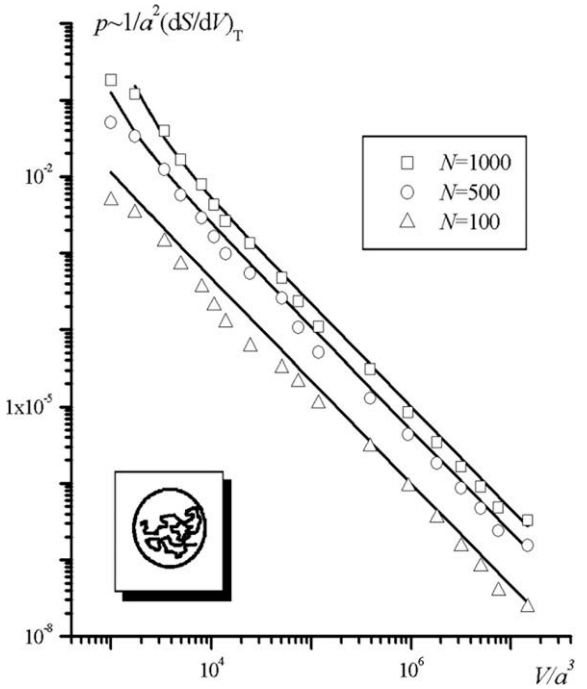

Fig. 14. Pressure exerted on an inner wall of spherical cavity by a confined polymer coil as a function of cavity volume V for different N values (as indicated in figure).

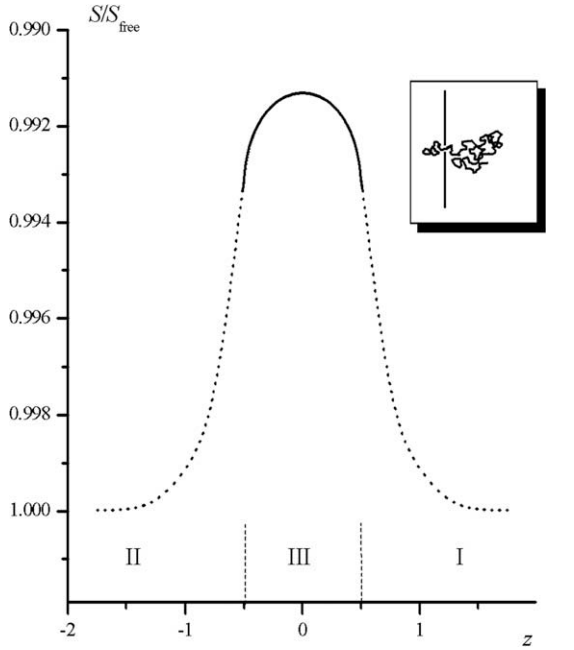

Fig. 15. The relative entropy profile for the entire process of chain transportation through a small hole in a flat wall from its one side to another (i.e. including the approach to, threading and departure from the wall), $N = 1000$.

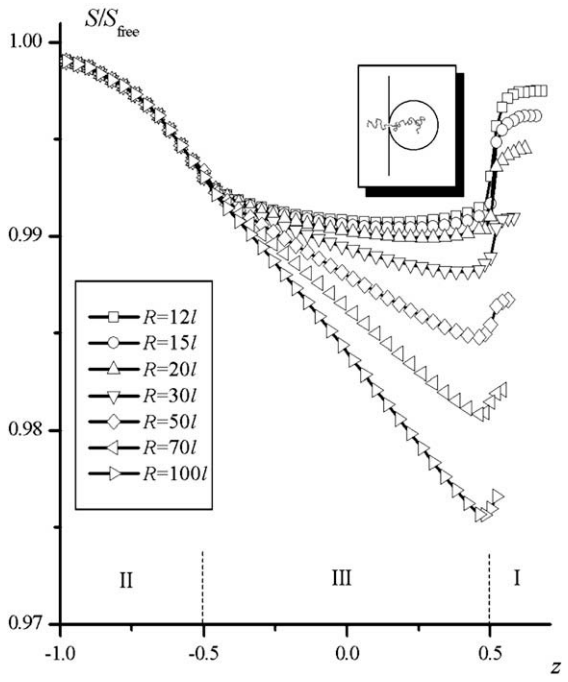

Fig. 16. Relative entropy profiles for the entire process of chain transfer from spherical cavities of different radii (as indicated in figure) into the half-space, $N = 1000$.

A comparison of quantitative dependencies of the conformational entropy on the translocation coordinate presented in Figs. 15 and 16 with the schematic predictions of the entire $S = f(z)$ relationship [30] shows the agreement of both data sets. Although the curve shapes are slightly different, they exhibit relatively high entropies at equilibrium states before and after the escape (S_I, S_{III}) and the minimum (S_{II}) between them. The difference $S_I - S_{III}$ is a measure of the difference between equilibrium or meta-equilibrium chemical potentials of polymers located at the donor or recipient space.

The thermodynamic description of the translocation (Figs. 3 and 5) also agrees with those obtained by the theoretical [23,35,50,51] and simulation (the MC method [31], the PERM method [21]) calculations of the free energy of the system as well as with the probabilities of steps of the translocation [52,53]. It seems that the differences between the results published in different papers are only consequences of different model properties (the inclusion of the excluded volume effect, different coordination numbers etc.). However, the results presented in [21,23,31,35,50–53] do not cover the whole $S = f(z)$ dependence. They are limited only to the pure translocation process in which the polymer chain is in contact with the hole and do not refer to the approach and retreat of polymer to/from the hole. As a consequence of the unified coordinate system of the translocation and approach/retreat processes, the model presented here allows us to obtain the entire entropy profile (Figs. 15 and 16).

In is noticeable that our calculations were performed for the reversible process, which is manifested by the fact that the conformational entropies take the maximum values at each step of the translocation. This assumption is exact only for the initial and final step of the translocation. For the fast translocation driven by the strong external force this assumption may fail, since the parts of the chain in the donor and recipient space do not have to reach the equilibrium state [54–58]. In such a case the entropy minimum should be even deeper than those observed in Figs. 15 and 16.

4. Concluding remarks

The conformation of a linear flexible polymer molecule in the course of the translocation through the hole in the impenetrable interfaces of different curvatures has been studied. The study addresses the problem in the athermal limit, in which only excluded volume interactions are considered. The polymer chain was modelled as a self-avoiding walk (SAW) on a cubic lattice. The segment positions in the lattice were chosen by the (1 1 2) algorithm which facilitates the location of chains in very tight environment. The equation of state of a macromolecule confined in a small cavity was proposed. The force necessary for approaching the polymer coil to the surface and the force exerted by the chain attached to the surface were determined and discussed. The entropy changes accompanying the translocation of the polymer molecule through a small hole in a number of systems of different geometries were calculated, and the equations describing the chain entropy and the thermodynamic force acting along the chain during the translocation were formulated. It was found that the height of the entropy barrier, which the translocating chain has to overcome, is comparable in size with that opposing the approach of the terminal segment of the chain to the interface. The height of the barrier can be reduced by an entropic pressure which arises when a macromolecule is confined in a cavity.

Acknowledgment

The work was partially supported by the Scientific Network – Surfactants and Dispersed Systems in Theory and Practice SURUZ (INCO-CT-2003-003355).

References

[1] Agarraberes FA, Diece JF. Biochim Biophys Acta 2001;1513:1.
[2] Schatz G, Dobberstein B. Science 1996;271:1519.
[3] Chen I, Christie PJ, Dubnau D. Science 2005;310:1456.
[4] Simon SM, Blobel G. Cell 1991;65:371.
[5] Tseng Y-L, Liu J-J, Hong R-L. Mol Pharmacol 2002;62:864.
[6] Nakane JJ, Akeson M, Marziali A. J Phys Condens Matter 2003;15:R1365.
[7] Zebirath J, Orelli S, Wang Y. Polymer 2005;46:10450.
[8] Slater GW, Guillouzic S, Gauthier MG, Mercier J-F, Kenward M, McCormic LC, et al. Electrophoresis 2002;23:3791.
[9] Matysiak S, Montesi A, Pasquali M, Kolomeisky AB, Clementi C. Phys Rev Lett 2006;96:118103.
[10] Randel R, Loebl H, Matthai CC. Macromol Theory Simul 2004;13:387.
[11] Kasianowicz JJ, Brandin E, Branton D, Dealer DW. Proc Natl Acad Sci USA 1996;93:13770.
[12] Tian P, Smith GD. J Chem Phys 2003;119:11475.
[13] Muthukumar M. J Chem Phys 1999;111:10371.
[14] Matsuyama A. J Chem Phys 2004;121:8098.
[15] Kong CY, Muthukumar M. J Chem Phys 2004;120:3460.
[16] Cacciuto A, Luijten E. Phys Rev Lett 2006;96:238104.

[17] Sakaue T, Raphaël E. Macromolecules 2006;39:2621.
[18] Milchev A, Binder K, Bhattacharya A. J Chem Phys 2004;121:6042.
[19] Luijten E, Cacciuto A. Comp Phys Commun 2007;177:150.
[20] Inamdar MM, Gelbart WM, Philips R. Biophys J 2006;91:441.
[21] Shen Y, Hang L. Polymer 2007;48:3593.
[22] Baumgärtner A, Skolnick J. Phys Rev Lett 1995;74:2142.
[23] Sung W, Park PJ. Phys Rev Lett 1996;77:783.
[24] Kong CY, Muthukumar M. Electrophoresis 2002;23:2697.
[25] Huopaniemi I, Luo K, Ala-Nisssila T, Ying SC. J Chem Phys 2006;125:124901.
[26] Qian J, Lu ZY, Li Z-S. Polymer 2007;48:3601.
[27] Sousa AF, Pais AACC, Linse P. J Chem Phys 2005;122:214902.
[28] Luo K, Ala-Nissila T, Ying S-C. J Chem Phys 2006;124:034714.
[29] Luo M-B. Polymer 2005;46:5730.
[30] Muthukumar M. Phys Rev Lett 2001;86:3188.
[31] Chern SS, Cardenas AE, Coalson RD. J Chem Phys 2001;115:7772.
[32] Loebl HC, Randel R, Goodwin SP, Mathai CC. Phys Rev E 2003;67:041913.
[33] Xie Y, Yang H, Yu H, Shi Q, Wang X, Chen J. J Chem Phys 2006;124:174906.
[34] Sikorski A, Romiszowski P. J Mol Model 2005;11:379.
[35] Kejian D, Furu Z, Dongquin C, Zengliang Y. Biochem Biophys Res Commun 2006;341:139.
[36] Lubensky DK, Nelson DR. Biophys J 1999;77:1824.
[37] Kantor Y, Kardar M. Phys Rev E 2004;69:021806.
[38] Muthukumar M. J Chem Phys 2003;118:5174.
[39] Frenkel D. Introduction to Monte Carlo methods. In: Attig N, Binder K, Grubmüller H, Kremer K, editors. Computational soft matter: from synthetic polymers to proteins, lecture notes, vol. 23. Jülich; 2004. p. 29–60.
[40] Zhao D, Huang Y, He Z, Qian R. J Chem Phys 1996;104:1672.
[41] Nowicki W, Nowicka G, Narkiewicz-Michałek J. Polymer 2009;50:2161.
[42] Sokal AD. In: Binder K, editor. Monte Carlo and molecular dynamics simulations in polymer science. New York: Oxford University Press; 1995.
[43] Gan HH, Tropsha A, Schlick T. J Chem Phys 2000;113:5511.
[44] Skolnick J, Kolinski A. Adv Chem Phys 1990;78:223.
[45] Nowicki W. Macromolecules 2002;35:1424.
[46] Bickel T, Jeppesen C, Marques CM. Eur Phys J E 2001;4:33.
[47] Lipowsky R, Döbereiner H-G, Hiergeist C, Indrani V. Physica A 1998;249:536.
[48] Lipowsky R. Colloids Surf A Physicochem Eng Aspects 1997;128:255.
[49] Tribet C, Vial F. Soft Matter 2008;4:68.
[50] Chuang J, Kantor Y, Kardar M. Phys Rev E 2001;65:011802.
[51] Park PJ, Sung W. Phys Rev E 1998;57(1):730.
[52] Cifra P. Macromolecules 2005;38:3984.
[53] Cifra P. J Chem Phys 2006;124:024706.
[54] Panja D, Barkema GT, Ball RC. J Phys Condens Matter 2007;19:432202.
[55] Panja D, Barkema GT, Ball RC. J Phys Condens Matter 2008;20:075101.
[56] Vocks H, Panja D, Barkema GT, Ball RC. J Phys Condens Matter 2008;20:095224.
[57] Dubbeldam JLA, Milchev A, Rostiashvili VG, Vilgis TA. Europhys Lett 2007;79:18002.
[58] Dubbeldam JLA, Milchev A, Rostiashvili VG, Vilgis TA. Phys Rev E 2007;76:010801.